Microscopic approach to the alpha-particle-nucleus optical potential

H. Leeb
Institut für Kernphysik, Technische Universität Wien, A-1020 Wien, Austria
and Institut für Kernphysik, Kernforschungsanlage Jülich, D-5170 Jülich, Federal Republic of Germany

F. Osterfeld
Institut für Kernphysik, Kernforschungsanlage Jülich, D-5170 Jülich, Federal Republic of Germany
(Received 1 February 1985)

A microscopic model for the alpha-particle-nucleus optical potential is presented and applied to α-^{40}Ca scattering. Starting with the M3Y force as the basic nucleon-nucleon interaction, the single-channel contribution to the optical potential is calculated by means of the fish-bone model which treats the antisymmetrization between the projectile and the target nucleus in an approximate way. The applicability of the fish-bone model to the α-^{40}Ca system is tested by comparison of resonating group calculations with fish-bone model calculations. The potential terms arising from the coupling of the elastic channel to other reaction channels have been calculated in the framework of the nuclear structure approach using random-phase approximation transition densities for intermediate excited states. The elastic scattering cross sections calculated from the microscopic potentials reproduce gross structures of the experimental data. However, the model cannot account for the whole absorption.

I. INTRODUCTION

Elastic scattering of alpha particles from nuclei has been known to be a very important tool in nuclear physics for a long time. The description of the process in the framework of the optical model has been studied extensively. In particular, phenomenological and semimicroscopic analyses of excellent cross section data have been performed for α-^{40}Ca scattering.[1] Unfortunately, such analyses can give only poor information about the alpha-particle-nucleus potential for two reasons: (i) The alpha particle is strongly absorbed at the nuclear surface, leading, therefore, to potential ambiguities at small radii.[2] (ii) The optical potential is always nonlocal due to exchange terms and due to the coupling of the elastic channel to other reaction channels. For simplicity, however, phenomenological and semimicroscopic analyses are based on local potentials. This approximation works rather well for nucleon-nucleus scattering. In the case of composite particle systems, however, the nonlocality is an essential feature and can be simulated by local potentials only under severe approximations[3] which lead to ambiguities in the potential. This situation is not satisfactory, since the optical potentials are the main input to many other reaction calculations. Although all ambiguous potential solutions produce the same elastic cross section, they lead to rather different results in reaction calculations, and one has therefore to ask for physically reliable potentials.

Because of these circumstances, the microscopic calculation of the optical potential for composite particle scattering is motivated not only from theory but also from a practical point of view. Today, there exist many papers in which the real part of the alpha-particle-nucleus optical potential has been successfully calculated by folding some sort of nucleon-nucleon interaction into the projectile and target nucleus matter densities.[4–6] More sophisticated approaches stress the importance of the Pauli principle using the resonating group method to determine the real part of the optical potential.[7–9] In these calculations a phenomenological imaginary part is added to the real potentials in order to describe the elastic scattering cross sections. Only in the last few years have microscopic calculations of the imaginary part of the alpha-particle-nucleus potential been reported.[10–12] The results of these calculations are promising, although complete agreement with the experimental cross sections has not been achieved. However, concentrating on the imaginary part, these authors have paid less attention to the real part which, in any case, dominates the interaction.

In this paper we report a calculation of the α-^{40}Ca optical potential which treats the real as well as the imaginary part of the potential on a microscopic basis. The dominant contribution to the real part is given by the folding term which is calculated by using the fish-bone model.[13] This model takes the antisymmetrization between projectile and target nucleons approximately into account. The imaginary part is calculated within the nuclear structure approach[10–12,14] to the optical potential neglecting the Pauli principle. As in Refs. 11 and 12, the coupling of all energetically open inelastic channels described by random-phase approximation (RPA) wave functions are included.

This paper is organized as follows. In Sec. II the model is described. Since the fish-bone model was never applied to α-^{40}Ca scattering, Sec. III is devoted to test its applicability to this scattering system. In Sec. IV some calculational details are given. The results of our calculations for incident alpha-particle energies of $E=26.1$, 31.0, and 36.1 MeV are reported in Sec. V. Finally, Sec. VI contains a brief summary and conclusions.

II. THE MODEL

In contrast to the nucleon-nucleus system there does not exist a unique definition of the optical potential for composite particle scattering on the basis of a many-body field theory. Therefore, one has to start from the formal derivation of the optical potential given by Feshbach[15]

$$U_{\rm opt}(\mathbf{r},\mathbf{r}')=\langle \mathbf{r}\Psi_A\Psi_B \mid PVP\mathscr{A} \mid \mathbf{r}'\Psi_A\Psi_B\rangle + \left\langle \mathbf{r}\Psi_A\Psi_B \left| PVQ\frac{1}{E-QHQ}QVP\mathscr{A} \right| \mathbf{r}'\Psi_A\Psi_B \right\rangle , \tag{1}$$

where P denotes the projection operator onto the elastic channel and $Q\equiv 1-P$. The elastic channel is characterized by the antisymmetrized ground state wave functions Ψ_A and Ψ_B of the target and projectile, respectively, together with the relative distance $\mathbf{r}(\mathbf{r}')$ between the two colliding nuclei. In Eq. (1), V is the microscopic interaction between the target and projectile nucleons and $\mathscr{A}$ is the antisymmetrization operator of the complete scattering system.

The first term of Eq. (1) is a folding term and corresponds to the resonating group potential when only one channel (the elastic channel) is considered. Describing the direct potential contribution to the elastic channel, this term dominates the optical potential and has been the subject of many publications. Due to the exact treatment of the antisymmetrization, the calculations become rather lengthy and, hence, are only feasible for certain simple systems like the α-α, α-^{16}O, α-^{40}Ca, etc. In order to also treat more complicated systems and to reduce the calculational effort, one has to look for suitable approximations which are simple but nevertheless contain the essential features of the resonating group method. Recently, Schmid[13] proposed the fish-bone model, which seems to fulfill these requirements.

In the fish-bone model one represents the resonating group exchange kernel on the basis of norm-kernel eigenstates $u_{p,\nu}$.[16] Here, p labels the partial waves and ν is a counting index for the norm-kernel states with given p. If one neglects a certain group of interaction terms, one obtains a very simple approximation to the resonating group potential which still retains the most important effects of antisymmetrization.[13] In partial-wave projection the first term of Eq. (1) becomes

$$\langle \mathbf{r}\Psi_A\Psi_B \mid PVP\mathscr{A} \mid \mathbf{r}'\Psi_A\Psi_B\rangle^{(p)}=V_1^{(p)}(r,r')\sim V_D^{(p)}(r)\delta(r-r')-\sum_\mu\sum_\nu u_\mu^{(p)}(r)\langle u_{p\mu} \mid T^{(p)}+V_D^{(p)}-E \mid u_{p\nu}\rangle M_{\mu\nu}^{(p)}u_\nu^{(p)}(r') , \tag{2}$$

where T denotes the kinetic energy operator and $V_D^{(p)}$ the direct local part of the resonating group potential. The fish-bone matrix $M_{\mu\nu}^{(p)}$ is easily constructed by the norm-kernel eigenvalues $\eta_{p,\nu}$,

$$M_{\mu\nu}^{(p)}=\eta_{p,\min\{\mu,\nu\}} . \tag{3}$$

The terms neglected in the fish-bone model can be partly compensated for by renormalizing the basic nucleon-nucleon interaction. This has been shown for light cluster systems by several authors.[17–20] The extension to α-^{40}Ca is straightforward and will be discussed briefly in the following section.

Investigations of three-cluster systems[21–23] suggest the use of an off-shell transformation in order to reduce Pauli-induced three-body forces. With regard to applications of the optical potentials in reaction calculations, where Pauli-induced three-body forces will occur, we have used the off-shell transformed version of the fish-bone model.[13] The transformation modifies only the fish-bone matrix $M^{(p)}$ slightly to $\overline{M}^{(p)}$,

$$\overline{M}_{\mu\nu}^{(p)}=1-\frac{1-M_{\mu\nu}^{(p)}}{[(1-\overline{\eta}_{p,\nu})(1-\overline{\eta}_{p,\mu})]^{1/2}} , \tag{4a}$$

with

$$\overline{\eta}_{p,\nu}=0 \quad \text{if } \nu\le n^{(p)} \qquad =\eta_{p,\nu} \quad \text{if } \nu>n^{(p)} . \tag{4b}$$

Here, $n^{(p)}$ is the number of completely Pauli-forbidden states in the partial wave p.

The second term of Eq. (1) describes the coupling of the elastic to all nonelastic channels. Neglecting antisymmetrization and considering second order contributions to the optical potential with respect to the effective projectile-target nucleon interaction, only the imaginary part of Eq. (1) is given by[24]

$$W_2(\mathbf{r},\mathbf{r}')=\mathrm{Im}\sum_N \langle \mathbf{r}\Psi_A \mid V_{nB} \mid \mathbf{r}\Psi_N\rangle g_N(\mathbf{r},\mathbf{r}') \times\langle \mathbf{r}'\Psi_N \mid V_{nB} \mid \mathbf{r}'\Psi_A\rangle , \tag{5}$$

where Ψ_N denotes the intermediate target excited states of energy E_N. $g_N(\mathbf{r},\mathbf{r}')$ is the intermediate projectile Green's function calculated at the energy $E-E_N$, and V_{nB} is the projectile target-nucleon interaction. Expression (5) is treated in the same way as in Refs. 11 and 25. In our calculations we have restricted the sum over N in Eq. (5) to all energetically open inelastic channels.

The contribution of the second term of Eq. (1) to the real part of the optical potential can be formulated similar to expression (5). But now, one has to sum over all energetically open and closed channels, respectively. Calculations[26] show that the sum over the closed channels converges in the case of the real part $V_2(\mathbf{r},\mathbf{r}')$ of the second order optical potential only very slowly,[26] thus increasing the numerical effort greatly. On the other hand, restricting the sum to open channels only does not yield a reliable approximation to $V_2(\mathbf{r},\mathbf{r}')$. Hence, we have simply neglected $V_2(\mathbf{r},\mathbf{r}')$ in our final calculations knowing that the error made by this approximation should be only of the order of 10%, since the real part of the optical potential is dominated by V_1.

III. THE FISH-BONE MODEL FOR α-^{40}Ca

In analogy to previous papers,[10–12] we consider the α-^{40}Ca scattering in order to test the model proposed in Sec. III. It is obvious that in our calculations the fish-bone potential will play an essential role. Until now there existed no experience with the α-^{40}Ca fish-bone optical potential because all applications have been restricted to lighter cluster systems. Hence, a brief test of the applicability of this potential to the α-^{40}Ca scattering is required.

Following Ref. 17 we make a comparison with available resonating group calculations.[7,9] As a reference calculation we use the work of Sünkel,[7] which is based on a two-nucleon interaction of near Serber mixture (80%) without hard or soft core.[27] We assumed an oscillator model for both the α particle and the ^{40}Ca nucleus with a width parameter of $\beta=0.25$ fm^{-2} in order to obtain the correct rms radius of ^{40}Ca. To compare the fish-bone with the resonating group model we take $V_D^{(p)}$ in Eq. (2) to be the local part of the resonating group potential[9] using the same parameters as in Ref. 7.

As a criterion for the quality of the first order potential we consider the rotational bands of ^{44}Ti which can be interpreted as quasimolecular states of the α-^{40}Ca system. Resonating group calculations[7,9] describe those resonances quite well. The fish-bone optical model shows a rotational band, too. However, there exists an additional even-odd splitting (Fig. 1) similar to the α-^{16}O system. This deficiency can be compensated for by introducing a Majorana term in $V_D^{(p)}$,

$$V_D^{(p)}(r)=V_{\rm loc}(r)[a+bP^r] \ . \tag{6}$$

Here, $V_{\rm loc}$ is the local resonating group potential for pure Serber mixing and P^r is the Majorana exchange operator

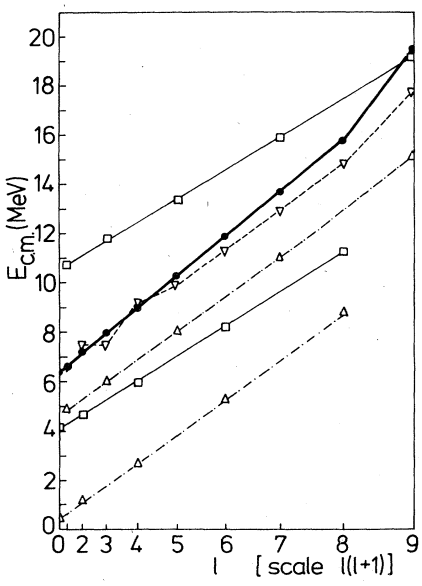

FIG. 1. Comparison of experimental and calculated rotational bands in ^{44}Ti. ●——, experiment; ▽ — — —, resonating group model; □——, fish-bone optical model; and △—·—·—·, orthogonality condition model using the local resonating group potential of 75% Serber mixture (Ref. 27).

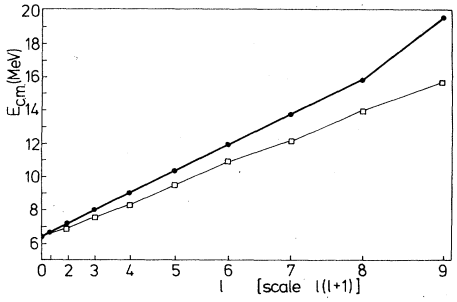

FIG. 2. Comparison of experimental and calculated rotational bands in ^{44}Ti. ●——, experiment; □——, fish-bone optical model using the local resonanting group potential with a Majorana term.

which interchanges the positions of the α and the ^{40}Ca cluster. The origin of this term has been discussed in Ref. 17. Using $a=0.762$ and $b=-0.036$ we obtain quite good agreement between theory and experiment (Fig. 2).

At this point it seems appropriate to make some remarks on features of the α-^{40}Ca fish-bone potential in comparison with the orthogonality condition model of Saito.[28] From Fig. 1 it can be seen that the rotational band of the orthogonality condition model using the same basic interaction lies about 2 MeV below that of the fish-bone optical potential. This indicates that the partly-Pauli-forbidden states, which are taken into account in the fish-bone model, give rise to some sort of barrier. Such an effect has been observed in light cluster systems and has led to the concept of a Pauli barrier.[29] Furthermore, there appears a change in the slope of the rotational band (Fig. 1). The increased moment of inertia in the fish-bone optical model is directly connected with the displacement of the wave functions to greater radii by partly-Pauli-forbidden states.

IV. CALCULATIONS

A. The folding potential V_F

In the preceding section it was pointed out that the fish-bone model reproduces the rotational spectrum of ^{44}Ti rather well. This property of the α-^{40}Ca fish-bone model Hamiltonian gives us some confidence that it is also suited to describe the α-^{40}Ca scattering in the single channel approximation (in analogy to the α-^{16}O system[17]). Starting from the M3Y effective nucleon-nucleon interaction of Bertsch *et al.*,[30]

$$v_{00}^{\rm M3Y}(r)=\left[6315\frac{e^{-4r}}{4r}-1961\frac{e^{-2.5r}}{2.5r}\right] \text{ MeV} \ , \tag{7}$$

V_F was obtained by folding $v_{00}^{\rm M3Y}$ into the ground state density distributions of ^{40}Ca (Ref. 31) and the α particle.[32] Then we multiplied the folding potential with a parity dependent normalization factor N in order to construct the direct potential V_D of the fish-bone model. The normalization factor was adjusted to reproduce the $J^\pi=0^+$ and $J^\pi=1^-$ resonances at $E_{\rm c.m.}=6.41$ MeV and 6.67 MeV, respectively. Thus the direct potential $V_D^{(p)}$ has the form

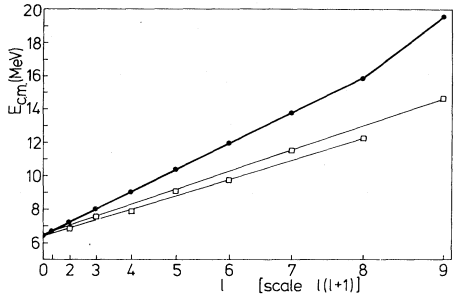

FIG. 3. Comparison of experimental and calculated rotational bands in ^{44}Ti. ●——, experiments; □——, fish-bone optical model using a folding potential calculated with the M3Y force (Ref. 30).

$$V_D^{(l)}(r)=[0.8713-0.0424(-1)^l]V_F(r)\ , \tag{8}$$

where l is the orbital angular momentum quantum number. Figure 3 shows the reproduction of the rotational bands by using this direct potential.

B. The intermediate Green's functions

The Green's function describing the propagation of the system in intermediate states was generated from the fish-bone potential V_1. Due to the nonlocality of V_1, an additional difficulty occurs because the Green's function in partial-wave expansion loses its simple separable form, thus increasing the numerical effort greatly. In order to reduce the computer time we have calculated the Green's function only in energy steps of 2.5 MeV and have then taken for every intermediate channel the propagator of the nearest energy value calculated. The numerical calculations were performed with the code GREFUL.[33] A phenomenological imaginary part of 0.01 $V_F(r)$ was added to the direct potential $V_D^{(l)}$ in order to damp potential resonances, thus simulating an energy averaging of the optical potential. For further information on this imaginary part we refer to Ref. 25.

C. Calculation of W_2

The second order potential is calculated as described in Ref. 11 using ^{40}Ca RPA vectors[34] for the intermediate states Ψ_N in Eq. (5). These vectors were obtained from a $3\hbar\omega$ basis including multipolarities $\lambda \leq 6$. All open inelastic channels were included in the sum of Eq. (5).

A very important input to our calculations is the α-target nucleon (n) interaction $V_{n\alpha}$. We use the same $V_{n\alpha}$ as in previous papers,[11,12]

$$V_{n\alpha}=N_{n\alpha}(-310.1e^{-0.422r^2}+319.2e^{-0.505r^2})\ , \tag{9}$$

which was derived by folding the M3Y force, Eq. (7), into the α-particle ground state density distribution. For the normalization factor we take the parity independent factor of Eq. (8), $N_{n\alpha}=0.8713$, in order to have consistent interactions in the first and second terms of the optical potentials. This normalization is consistent with inelastic cross-section calculations for ^{40}Ca$(\alpha,\alpha')^{40}$Ca* ($3^-, E_x=3.73$ MeV) at $E_\alpha=30$ MeV which require a renormalization factor of $N_{n\alpha}=0.7$.

V. RESULTS

A. The second order potential W_2

The second order potential is highly nonlocal. In order to get a feeling for the structure of the nonlocal potential we show in Fig. 4 perspective drawings of $W_2(\mathbf{r},\mathbf{r}')$ for zero angle $\mathbf{r}\cdot\mathbf{r}'=rr'$ at several energies. From these graphs it is obvious that W_2 tends to a local potential but there are also large nonlocal contributions. The second order potential for alpha-particle-nucleus scattering is highly dependent on the intermediate Green's function.[11] In order to give an impression of the importance of the intermediate Green's function we also show in Fig. 4 the imaginary part at $E_L=31$ MeV calculated in Ref. 11. This calculation differs only in the use of different potentials generating the propagators and a different normalization of the α-target nucleon interaction. The latter is mainly responsible for the different size of the potential at

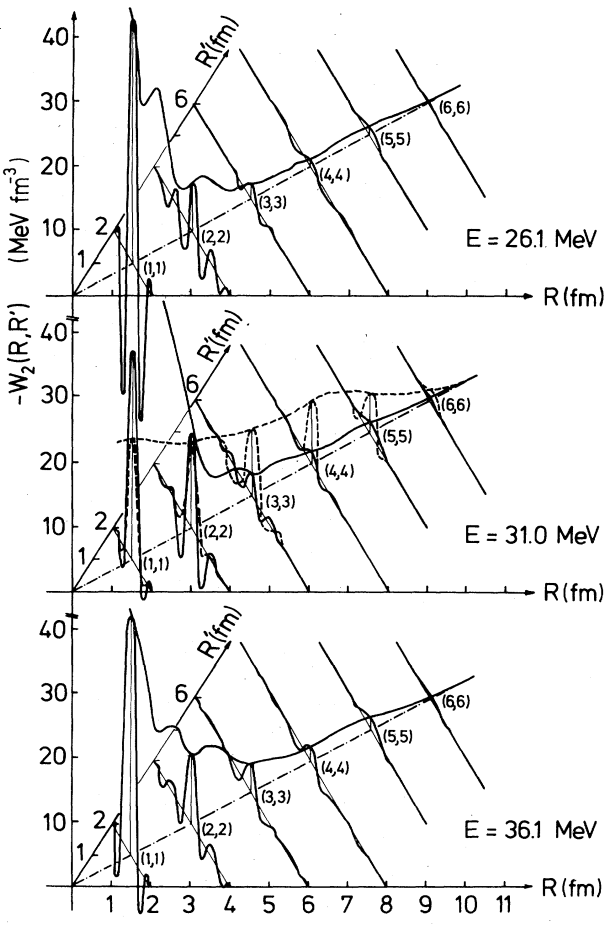

FIG. 4. Perspective drawing of the nonlocal second order imaginary optical potential $W_2(\mathbf{R},\mathbf{R}')$ for zero angle $\mathbf{R}\cdot\mathbf{R}'=RR'$ at several incident alpha particle energies (solid line). At 31.0 MeV the dashed line denotes $W_2(\mathbf{R},\mathbf{R}')$ calculated in Ref. 11.

the nuclear surface.

A very interesting point is the energy dependence of the second order potential. However, due to the complex structure of the nonlocal potential it is rather difficult to fix it. If we restrict our considerations to the localization point $\mathbf{r}=\mathbf{r}'$, we observe an imaginary part at the nuclear surface which increases with increasing energy, thus indicating an increasing absorption. Due to the shielding effect of the absorption on the nuclear surface, the nonsystematic behavior of the imaginary potential at small radii should not influence the global trend of the absorption.

B. Calculation of the elastic differential cross sections

The complex structure of the nonlocal potentials requires a complete nonlocal calculation of the differential elastic cross sections.[12] Any localization procedure used in similar previous works[10,11] will lead to doubtful results. In Fig. 5 the theoretically calculated elastic differential cross sections are compared with experimental data[1] at several energies. In order to show the influence of the second order potential W_2 on the differential elastic cross sections we also show cross sections calculated with the first order fish-bone model alone. It is obvious that the inclusion of W_2 improves the agreement with experiment considerably. The gross structure of the angular distributions is well reproduced by the microscopic optical potential. In particular one obtains the characteristic energy behavior around 90° quite satisfactory. But looking on the absolute values, the theoretical cross sections are always too high, thus indicating too little absorption in our model. This deficiency is not surprising since we take into account only inelastic channels, but there is a large number of other open channels like, e.g., transfer reaction channels which will also considerably contribute to the absorption. The failure of the microscopic potentials in producing too little absorption is expressed also in the total nonelastic cross sections σ_{ne} displayed in Fig. 5. In comparison to phenomenological analyses,[1] only about 55% of the total absorption cross section is reproduced by our calculations.

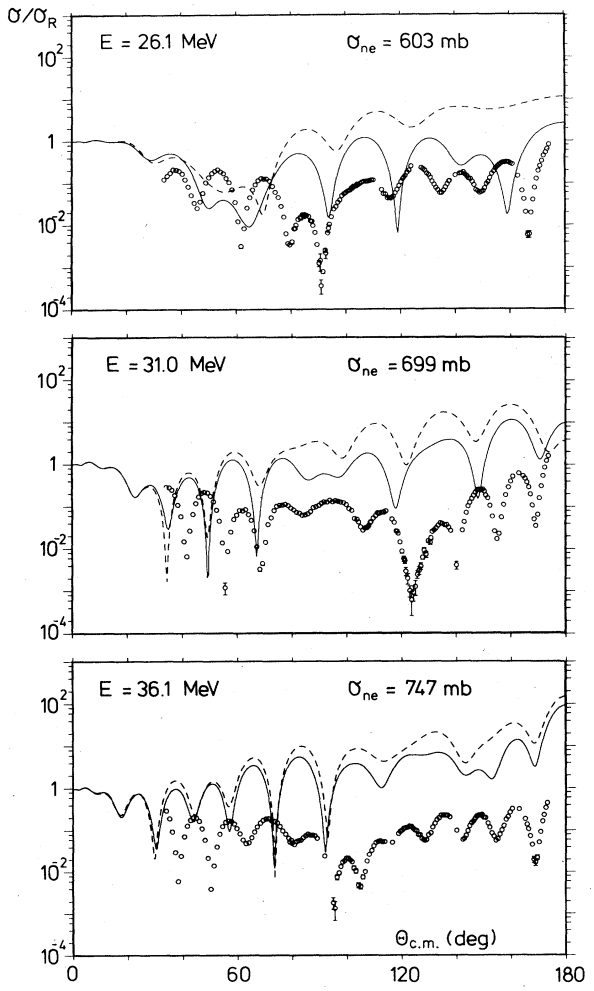

FIG. 5. Comparison of the calculated elastic differential cross sections with the experimental data of Ref. 1. ——, calculation with first and second order potential. — — —, calculation using only the first order fish-bone potential.

C. Pauli principle and second order potential

The neglect of various reaction channels is not the only reason for the too small absorption, because previous calculations[12] which include the same number of intermediate states obtain larger values for σ_{ne}. As mentioned above, the main difference between our calculations and previous ones[12] is the use of an intermediate Green's function which in our case is generated from the nonlocal fish-bone optical potential. The structure of the ground states of projectile and target is an essential input to this fish-bone model via the norm-kernel eigenvalues. In our special system, both the alpha particle and the ^{40}Ca nucleus have closed shells in their ground states. In this case the number of totally forbidden states and the effect of partly-Pauli-forbidden states become maximal in the α-Ca cluster decomposition of the $A=44$ nucleon system. In intermediate states, however, at least one particle is excited, and we have no closed shell any longer. Hence, generally the number of totally-Pauli-forbidden states is reduced, and also the effect of partly-Pauli-forbidden states on the propagator decreases. Therefore, the propagation probability of the projectile in intermediate states will increase and, therewith, also the Green's function and its imaginary part.

An exact calculation would require the determination of the resonating group potential for every intermediate channel. The effort for such a calculation is not justified compared to the other assumptions made in our model. In order to get an estimate on the magnitude of this Pauli reduction we made a very rough calculation. We assumed that one nucleon of ^{40}Ca is highly excited and that the corresponding hole state of ^{40}Ca completely overlaps with one nucleon wave function of the α particle. In this case we have to apply the Pauli principle only to the ^{3}He-^{40}Ca system. We take the ^{3}He-^{40}Ca norm kernel together with the direct potential $V_D^{(l)}$ of Eq. (8) and construct the fish-bone model for intermediate states. Then we calculate the corresponding Green's function $G^{^3\mathrm{He}}$ for an energy of $E-E_N=10$ MeV which essentially corresponds to the

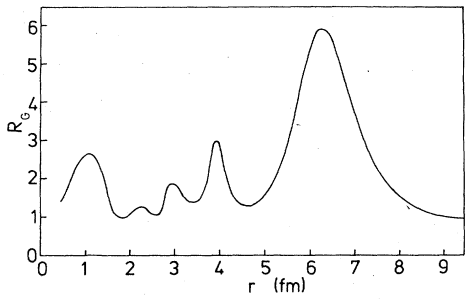

FIG. 6. Radial dependence of the ratio $R_G(r)$ at the localization point $\mathbf{r}=\mathbf{r}'$.

average energy of the propagating α particle in intermediate states. In Fig. 6 we show the ratio

$$R_G(r)=\frac{G^{^3\mathrm{He}}(\mathbf{r},\mathbf{r})}{G^{\alpha}(\mathbf{r},\mathbf{r})} \tag{10}$$

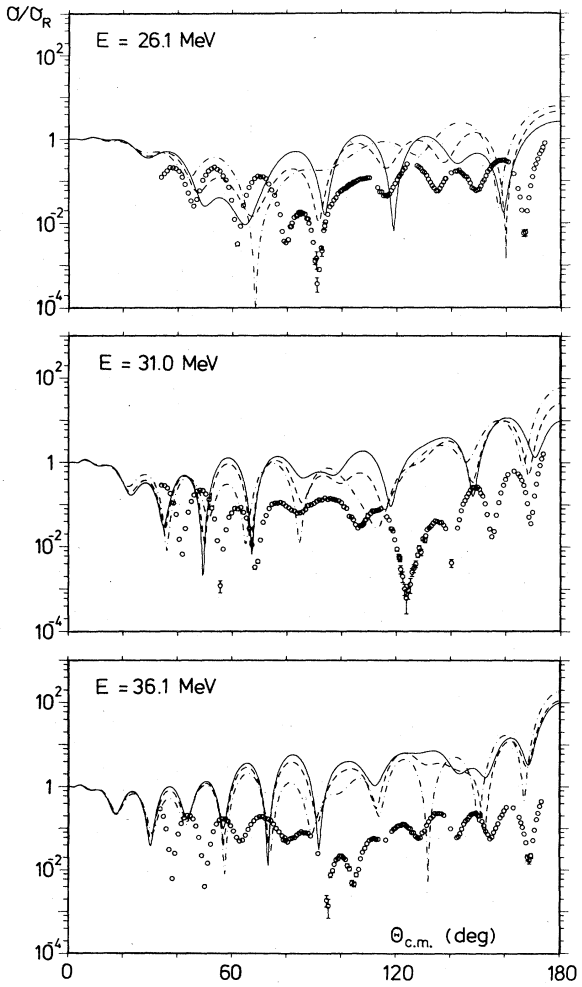

FIG. 7. Comparison of the experimental elastic differential cross sections of Ref. 1 with microscopic calculations using different scaling factors $\overline{R}$ for the second-order imaginary potential. ——, $\overline{R}=1$, — — —, $\overline{R}=2$, and $\overline{R}=6$.

at the localization point $\mathbf{r}=\mathbf{r}'$. Here, G^{α} denotes the Green's function which has been obtained by the fish-bone potential using the α-^{40}Ca (ground state) norm kernel. As expected, the ratio R_G is always greater than 1. Furthermore, we see that the correct treatment of the Pauli principle will affect the imaginary potential W_2 mainly at the nuclear surface. In Fig. 7 we show calculations of the differential cross sections where the imaginary potential W_2 has been multiplied by different factors $\overline{R}$. In particular, we have calculated the case $\overline{R}=2$ which corresponds to a mean value of $R_G(r)$ over the whole radial range and the case $\overline{R}=6$ which represents the maximum of $R_G(r)$. The resulting cross sections are strongly affected by the scaling factor $\overline{R}$, thus indicating the importance of the correct treatment of the Pauli principle in the intermediate channels. It might be accidental, but for the average value $\overline{R}=2$ an improvement in the reproduction of the gross structure is observed.

At this point it is opportune to discuss the promising results[11,12] obtained by local first order potentials. In both Refs. 11 and 12 shallow phenomenological first order potentials were used. A local potential can simulate a totally-Pauli-forbidden state by introducing additional bound states.[3] In our fish-bone model, however, there are for every partial wave more totally-Pauli-forbidden states than there are bound states in the shallow potentials used in Refs. 11 and 12. Therefore, one would expect that the propagation probability is overestimated.

VI. SUMMARY AND CONCLUSIONS

Starting from a nucleon-nucleon interaction we have calculated the nonlocal optical potentials for α-^{40}Ca scattering at 26.1, 31.0, and 36.1 MeV, using the nuclear structure approach. While the Pauli principle has been approximately taken into account in the first order term, we have omitted the structure of the α particle in the determination of the second order contributions. The nucleon-nucleon interaction was normalized in order to reproduce the rotational band in ^{44}Ti. For this purpose we have tested the applicability of the fish-bone optical potentials to α-^{40}Ca scattering and found similar features as in light cluster systems. The calculated second order potentials are highly nonlocal, and a comparison with a previous work[11] shows the sensitivity of the optical potentials to the intermediate Green's functions.

A comparison of our calculated differential cross sections with experimental data is quite satisfactory. Although there is no fitting parameter in our model (the renormalization of the nucleon-nucleon interaction has been fixed to reproduce the 0^+ and 1^- resonances of ^{44}Ti near 6.5 MeV) we successfully reproduce the gross structure of the differential cross sections. The theoretically determined potentials underestimate the absorption in general. There exist several reasons for this deficiency: (i) the noncorrect treatment of the Pauli principle in intermediate channels; (ii) the neglect of other energetically open reaction channels than inelastic channels, like, e.g., transfer channels which may contribute significantly to the absorption; it is likely that especially transfer processes contribute to the long range part of the absorption and thus

carry a large weight; (iii) the uncertainty in the second order real potential can also influence the absorption.

Concluding, one can say that the fish-bone model together with the nuclear structure approach is an effective tool to describe elastic α-^{40}Ca scattering at low energies. The complete nonlocal calculations eliminate the doubts connected with localization procedures. But there remain serious problems. First, one has to perform a Pauli-correct calculation of the second order imaginary part. Second, one has to include transfer channels, which most probably are dominantly responsible for the missing absorption. Furthermore, a consistent and complete calculation of the second order real potential is required. In spite of these problems we think that the model proposed is a further step towards a better microscopic understanding of alpha-particle-nucleus optical potentials.

ACKNOWLEDGMENTS

Discussions with Prof. E. W. Schmid and Prof. J. Speth in the early stage of this work are gratefully acknowledged. One of us (H.L.) wants to thank Prof. Speth for the hospitality extended to him at the Kernforschungsanlage Jülich and would like to acknowledge as well financial support from that institution.

[1]H. P. Gubler, U. Kiebele, H. O. Meyer, G. R. Plattner, and I. Sick, Nucl. Phys. **A351**, 29 (1981); Phys. Lett. **74B**, 202 (1978).
[2]G. Igo, Phys. Rev. Lett. **1**, 72 (1958); Phys. Rev. **115**, 1665 (1959).
[3]H. Leeb and E. W. Schmid, Z. Phys. A **296**, 51 (1980).
[4]G. R. Satchler and W. G. Love, Phys. Rep. **55**, 183 (1979).
[5]C. C. Morgan and D. F. Jackson, Phys. Rev. **188**, 1758 (1969).
[6]B. Sinha, Phys. Rep. **20**, 1 (1975).
[7]W. Sünkel, Phys. Lett. **65B**, 419 (1976).
[8]H. R. Fiebig and A. Weiguny, Z. Phys. A **279**, 275 (1976).
[9]H. Friedrich and K. Langanke, Nucl. Phys. **A252**, 47 (1975).
[10]N. Vinh Mau, Phys. Lett. **71B**, 5 (1977); N. Vinh Mau, *Microscopic Optical Potentials,* Vol. 89 of *Lectures Notes in Physics* (Springer, Berlin, 1979), p. 40.
[11]H. Dermawan, F. Osterfeld, and V. A. Madsen, Phys. Rev. C **25**, 180 (1982).
[12]H. Dermawan, F. Osterfeld, and V. A. Madsen, Phys. Rev. C **27**, 1474 (1983).
[13]E. W. Schmid, Z. Phys. A **297**, 105 (1980).
[14]N. Vinh Mau and A. Boussy, Nucl. Phys. **A257**, 295 (1976).
[15]H. Feshbach, Ann. Phys. (N.Y.) **19**, 287 (1962).
[16]M. Horiuchi, Suppl. Prog. Theor. Phys. **62**, 90 (1977).
[17]H. Leeb and E. W. Schmid, Z. Phys. A **298**, 113 (1980).
[18]R. Kircher and E. W. Schmid, Z. Phys. A **303**, 241 (1981).
[19]G. Spitz, K. Hahn, and E. W. Schmid, Z. Phys. A **303**, 209 (1981).
[20]M. Orlowski and E. W. Schmid, Z. Phys. A **306**, 51 (1982).
[21]E. W. Schmid, Z. Phys. A **302**, 311 (1981).
[22]H. Leeb and E. W. Schmid, Czech. J. Phys. **B32**, 213 (1982).
[23]E. W. Schmid, M. Orlowski, and Bao Cheng-guang, Z. Phys. A **308**, 237 (1982).
[24]C. L. Rao, M. Reeves, and G. R. Satchler, Nucl. Phys. **A207**, 182 (1973).
[25]F. Osterfeld, J. Wambach, and V. A. Madsen, Phys. Rev. C **23**, 179 (1981).
[26]F. Osterfeld and V. A. Madsen, Phys. Rev. C (in press).
[27]E. W. Schmid and K. Wildermuth, Nucl. Phys. **26**, 463 (1961).
[28]S. Saito, Prog. Theor. Phys. **41**, 705 (1969).
[29]S. Saito, E. W. Schmid, and M. Fiedeldey, Z. Phys. A **306**, 37 (1982).
[30]G. Bertsch, J. Borysowicz, H. McManus, and W. G. Love, Nucl. Phys. **A284**, 339 (1977).
[31]R. F. Frosch, R. Hofstadter, J. S. McCarthy, G. K. Nöldeke, K. J. Oostrum, M. R. Yearion, B. C. Clark, R. Herman, and D. G. Rowenhall, Phys. Rev. **174**, 1380 (1968).
[32]J. S. McCarthy, I. Sick, and R. R. Whitney, Phys. Rev. C **15**, 1396 (1976).
[33]H. Leeb and H. Markum, Comput. Phys. Commun. **34**, 271 (1985).
[34]S. Krewald and J. Speth, Phys. Lett. **74B**, 295 (1974).